A new method for the experimental simulation of surface crack formation in continuous casting

Article *in* La Metallurgia Italiana · April 2017

CITATIONS
2

READS
128

5 authors, including:

Sergiu Ilie
Voestalpine
45 PUBLICATIONS **206** CITATIONS
SEE PROFILE

Susanne Hahn
Primetals Technologies
18 PUBLICATIONS **449** CITATIONS
SEE PROFILE

A new method for the experimental simulation of surface crack formation in continuous casting

R. Krobath, C. Bernhard, S. Ilie, J. Six, S. Hahn

Transverse cracks on semi-finished continuously cast products can still present quality problems in the steel industry. The surface cracking phenomenon is complex and therefore often difficult to predict. At the Chair of Ferrous Metallurgy, Montanuniversität Leoben, a new testing method for determining the susceptibility to surface cracking according to the steel composition and cooling strategy was developed. The In-Situ Material Characterization – Bending (IMC-B) test enables the investigation of samples formed directly from the liquid and cooled according to a given temporal sequence. The samples form austenite grain structures with grain sizes similar to those at strand surfaces. At a specified time, a three-point bending test is performed, in which the sample is deformed at a constant temperature using a defined strain rate to a maximum strain. The maximum is determined according to the bending/straightening zone, and limited to a few percent. The bending process is controlled with a processing unit and simulated with the finite-element software Abaqus. The specimen surface is observed for cracks at a high magnification to detect even very small defects. The cracks are documented and analyzed with different techniques. Furthermore, the crack morphology is determined. Phase transformations according to the post-bending samples are simulated practically by high-temperature laser scanning confocal microscopy observations. Test series with construction steels of varying Nb contents are performed. The formation of surface cracks is strongly influenced by the bending temperatures (between 700°C and 950°C) and the Nb content, whereas the detected number of cracks is proportional to the Nb content. An investigation of the experiments with different maximum induced strains also shows a clear correspondence to the formation of surface cracks.

KEYWORDS: CONTINUOUS CASTING - TRANSVERSE CRACK FORMATION - MICROALLOYED STEEL - IMC-B TEST - IN-SITU HOT BENDING TEST

INTRODUCTION

Because surface defects on continuously cast semi-finished steel products can cause massive defects in the final sheets, it is important to determine the causes and locations of surface flaws. Transverse crack formation in particular is influenced by many factors. The tendency for transverse cracking is related to the material properties of the strand surface and the operating mechanical and thermal stresses throughout the casting process. In reviewing the secondary cooling zone, the unbending of the strand induces critical strains on the surface, reaching ~2%. The trigger for crack formation is a surface temperature promoting high embrittlement in this cooling zone, referred to as the second ductility trough. The material behavior can deteriorate further in the presence of mold defects, such as unusually large austenite grains, oscillation marks, or uneven strand surfaces [1-5]. The temperature range of the second ductility trough is generally determined by hot tensile tests, performed in the laboratory under inert atmospheres. The samples are pulled to rupture at different testing temperatures. The ductility is directly related to the measured reduction of area (RA) of the broken samples. Authors have named different critical RA-values as indicators for surface cracking. Mintz and You [6] determined that values of 30–40% were critical. In recent decades, many studies of hot tensile testing have been done; e.g., Schwerdtfeger [7] and Mintz

R. Krobath, C. Bernhard
Montanuniverstitaet Leoben, Austria

S. Ilie, J. Six
Voestalpine Stahl, Linz, Austria

S. Hahn
Primetals Technologies, Linz, Austria

[3] summarized particular factors that influenced the RA-values, demonstrating the potential for hot tensile tests in determining high-temperature material behavior. The curves can be used to adjust the casting parameters in continuous casting machines and the temperatures during unbending, which can be critical. However, constraints remain for the direct relation of RA-values to the strand surface.

Starting in the mold, the strand shell is characterized by a significant solidification structure where pre-damage artifacts (e.g., oscillation marks and segregations) can form. Under normal circumstances, tensile tests are performed with reheated samples; the austenite grain structures in these samples differ from those in the strand shell. Studies show significant influence of the direction in which the sample is obtained on the ductility; even when during preheating new austenite grain structures form [8]. This provides evidence of the importance of grain structure similarities for the experimental simulation of surface crack formation.

Significant differences are observed for the stress–strain state. In hot tensile testing, longitudinal strains cause sample rupture. For low RA-values, the strain before rupture remains high (~10% or more). As mentioned before, the strain prior to surface cracking in the unbending zone reaches only 2% for a material experiencing no constriction [2, 9, 10]. These high strains in laboratory experiments cause material phenomena that can influence the higher and lower flanks of the ductility curve. At higher temperatures, boundary migration occurs at increasing strains; this causes dynamic recrystallization. Dynamic recrystallization is the consequence of ductility recovery at higher temperatures [3, 11].

The causative high strains for this phenomenon are not present at the strand surface. The lower slope of embrittlement is caused by the γ-to-α phase transformation. More precisely, the start of the phase transition can be critical. If the A_{R3} temperature is reached, ferrite begins forming at prior austenite grain boundaries. Strain becomes concentrated on these ferrite films during deformation, thereby significantly lowering the ductility [2, 12]. Inducing strains in the material increases the A_{R3} temperature. This deformation-induced ferrite is more likely to form at higher strains, lower strain rates, and smaller austenite grain sizes [11, 13]. The described strain-induced phenomena during tensile testing can shift the second ductility trough, as determined by RA-temperature (T) curves. This can impede the direct application of RA-T curves for predicting surface crack formation in continuous casting.

During casting and cooling, the strand surface is not protected from scale formation, which could influence defect formation. However, laboratory experiments are performed under inert atmospheres, which prevent scaling.

At Montanuniversitaet Leoben, Chair of Ferrous Metallurgy, a new experimental method for determining the susceptibility to surface crack formation under continuous casting conditions was realized within the earlier Comet-K2 and K1-MET projects (In-situ Material Characterization–Bending test; IMC-B). This report describes the principle and procedure of the test. Furthermore, the results for a Nb-microalloyed construction steel and the influence of Nb content, deformation temperature, and induced strain are given.

EXPERIMENTAL PROCEDURE

The experiment can be divided into three main steps. It starts with the melting and solidification part. Furthermore, the solidified sample is cooled according to a given temporal sequence. At a specified time, the sample is deformed using a three-point bending test under isothermal conditions. This section describes the three steps in detail.

The test begins with the melting of the steel in an induction furnace. One advantage of the induction furnace is the opportunity to freely adjust the sample composition by adding elements with high purity. In addition, the furnace atmosphere can be set as air, an inert gas (Ar), or vacuum. This is important if low [N] values are needed in the melt. The steel composition is checked using an optical emissions spectrometer (OES) for accuracy. For similar solidification conditions, the casting temperature must be the same for every sample in the testing series. The alloy flows through the casting system into a special mold. This process is shown in 1. In the middle, the heat flux through the coating and the mold wall is presented. The powder coating with a defined thickness on the mold wall ensures similar heat losses from the solidifying steel for each sample. This is essential for inducing directional dendrite growth, which is shown for the sample in 1 – picture a). The structure coarsens with increasing distance from the sample surface. This also occurs in cast slabs [14, 15]. During solidification, typical phenomena such as segregations (also shown) and micropore formation occur. After solidification, the austenite grain structure evolves. In picture b), a Nital-etched sample reveals the prior austenite grain structure in the cross-section of the sample. The grain texture growing from the sample surface is fine. With increasing distance, coarsening is observed. Reiter et al. [16] investigated a similar coarsening of the austenite grains depending on the distance from the slab surface. This is caused by the longer time at higher temperatures with increasing distance from the slab surface. On the surface, the four investigated steels show similar grain sizes, whereas the coarsening effect depends strongly on the equivalent carbon content. For the appearance of surface cracking, the surface grain size is decisive. However, once a crack is formed, it can propagate along the columnar austenite grain boundaries [8]. Studies of hot tensile tests have shown that larger grain sizes negatively influence the ductility of specimens. The ductility trough is widened to higher and lower temperatures [17, 18, 19]. This indicates the importance of similarity in the austenite grain structures between the experimental specimen and the slab surface.

The present study shows the results of experiments with an Al deoxidized construction steel with a C content of 0.17 wt.%. To the standard composition, different amounts of Nb are added (1). This approach should reveal the influence of Nb to the formation of surface cracks in the investigated samples.

Tab. 1 - Steel compositions for the present test series

	C [wt.%]	Si [wt.%]	Mn [wt.%]	P [wt.%]	S [wt.%]	Al [wt.%]	Nb [wt.%]	N [ppm]
Steel 0Nb	0.17	0.4	1.55	0.01	<0.004	0.03	0.002	50
Steel 0.02Nb	0.17	0.4	1.55	0.01	<0.004	0.03	0.02	50
Steel 0.04Nb	0.17	0.4	1.55	0.01	<0.004	0.03	0.04	50

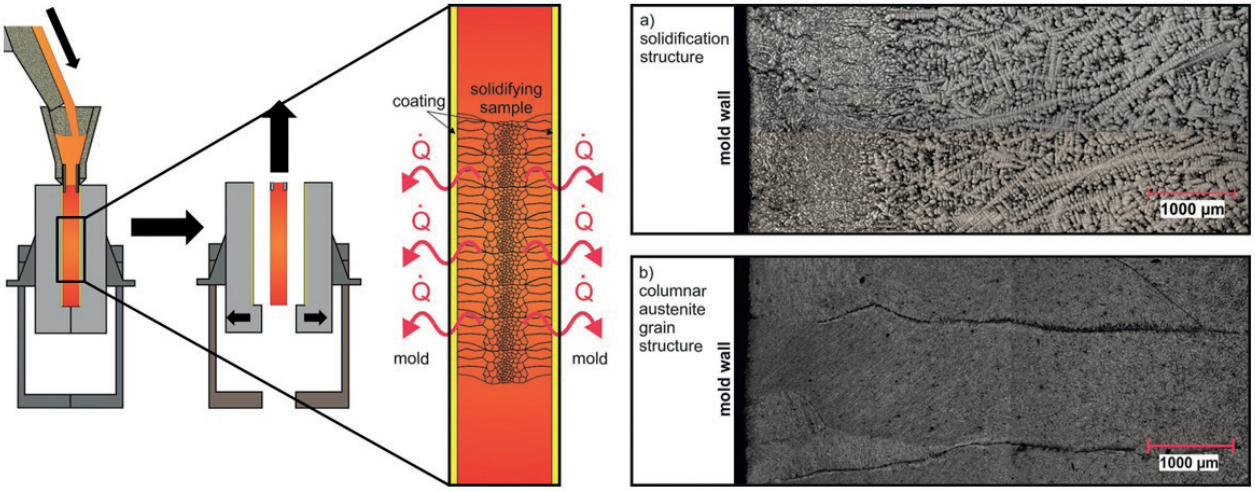

Fig. 1 - Schematic view of the casting and solidification process; picture a) – solidification structure, etched with Bechet and Beaujard; picture b) – visualized columnar austenite grain structure, Nital etching (3% HNO_3)

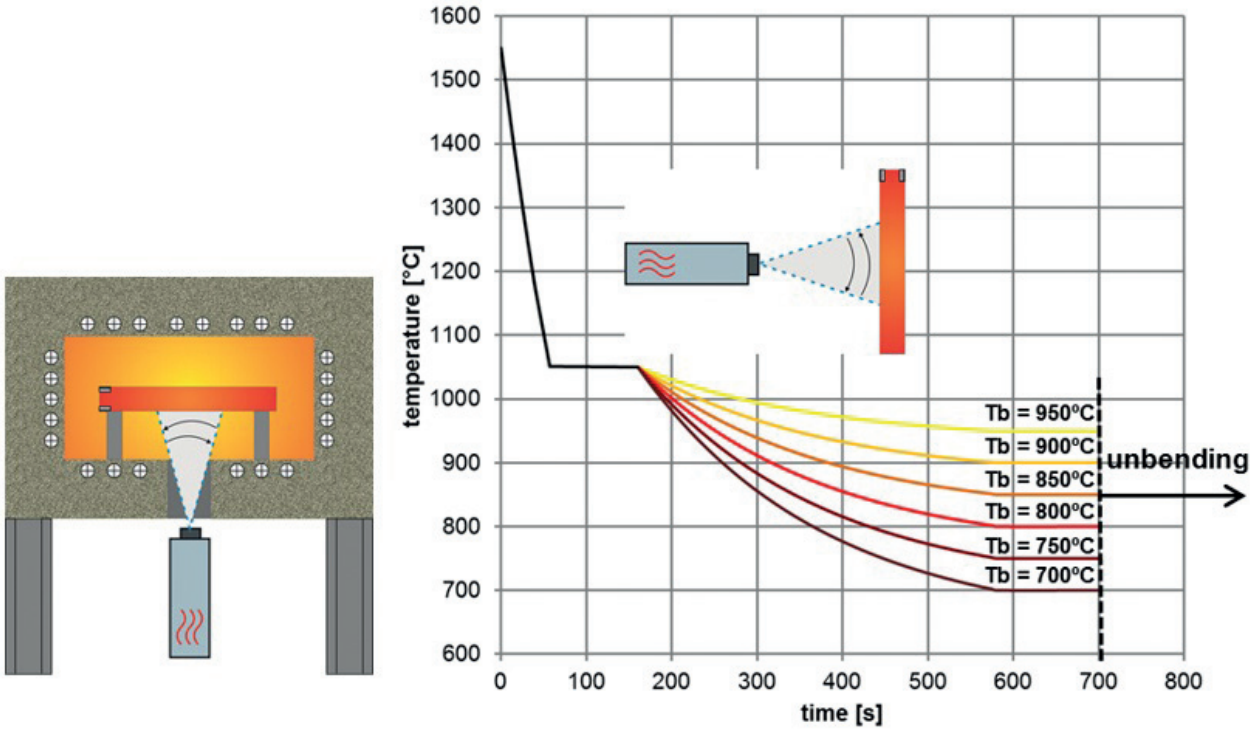

Fig. 2 - Temporal sequence for the present test series; six bending temperatures of 700 to 950°C

Surface quality of continuous casting products

The initial time in the mold regulates the surface temperature after stripping. Fig. 2 provides the temporal sequence for the performed experiments. After stripping, the sample surface temperature is immediately checked with a pyrometer. After 45 s of residual time in the mold, the sample surface reaches a temperature of ~1130°C. It cools in atmosphere to a temperature of 1050°C, at which point a homogenization step is implemented to the total time of 160 s. The sequence to this time is constant for each experiment. Therefore, differences in the precipitation state and the austenite grain structure are only influenced by the chemical compositions of the steels. Subsequently, the samples are cooled at various cooling rates. The varied rates are used to investigate the influence of different cooling rates in the secondary cooling zone on the formation of surface cracks during unbending. Continuous measurement of the surface temperature for every experiment during cooling is performed with a line-scanning system for the optical pyrometer, to obtain information for a large part of the sample surface. After 580 s, the samples reach the bending temperatures. Here, the sample temperatures are again homogenized until the total time of 700 s.

This cooling sequence is adjusted to match the calculated temperature profile of a slab cast with a thickness of 225 mm and a casting speed of 1.2 m/min [20]. The strand reaches the unbending zone at a total elapsed time of 700 s. The controlled cooling prior to this point and the six bending temperatures of 700 to 950 °C at 50-°C intervals can be called the second step of the test. The third part, which is the deformation of the sample adjusted to the loads in the unbending zone, follows. This is realized via a three-point bending test, performed isothermally to determine the influence of deformation temperature on the formation of transverse cracks with a constant stamp velocity. Fig. 3 shows, on the left-hand side, the schematic view of the isothermal three-point bending test. The chamber temperature is controlled with two thermocouples. To obtain information of the initiated stress–strain state depending on the deflection, the test is simulated by the finite element method (FEM) software Abaqus. A snapshot is presented in Fig. 3, middle. The stamp moves against the z-direction. The lower surface of the sample is deformed, following the behavior of the upper strand surface in the unbending section. For the test series listed in Tab.1, the maximum induced strain in the x-direction is ~1.5% with a strain rate of 6.10^{-4} s^{-1}. In Fig. 3, on the right-hand side, the side view of the deflection at room temperature is shown to remain very low. The force and movement of the stamp during the test is recorded with a data-acquisition processer. The samples are slowly cooled to room temperature after deformation. This decreases the thermal- and transformation (γ-to-α)-induced stresses during cooling and therefore decreases the possibility of crack formation after bending.

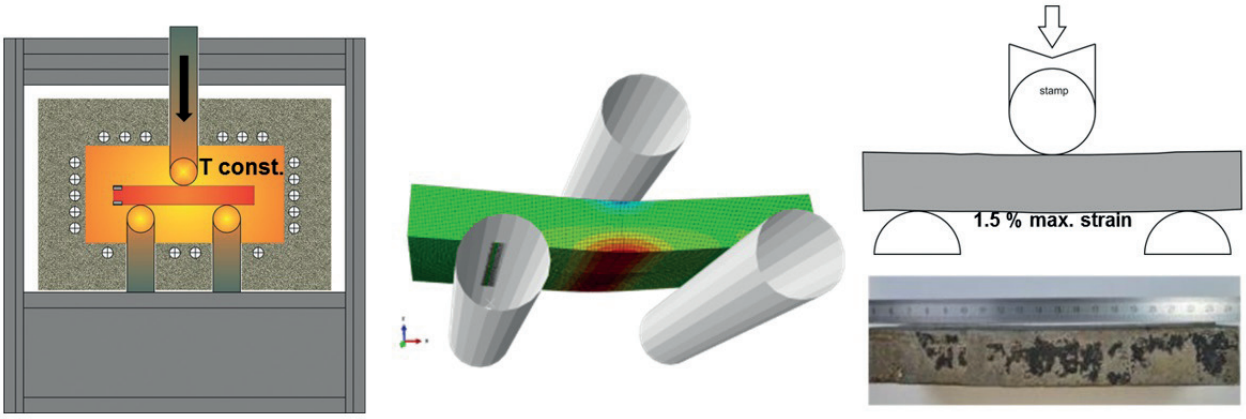

Fig. 3 - Left side: schematic view of the isothermal three-point-bending test; middle: snapshot of Abaqus simulation; right side: deflection of the sample at room temperature, maximum strain ~1.5 %

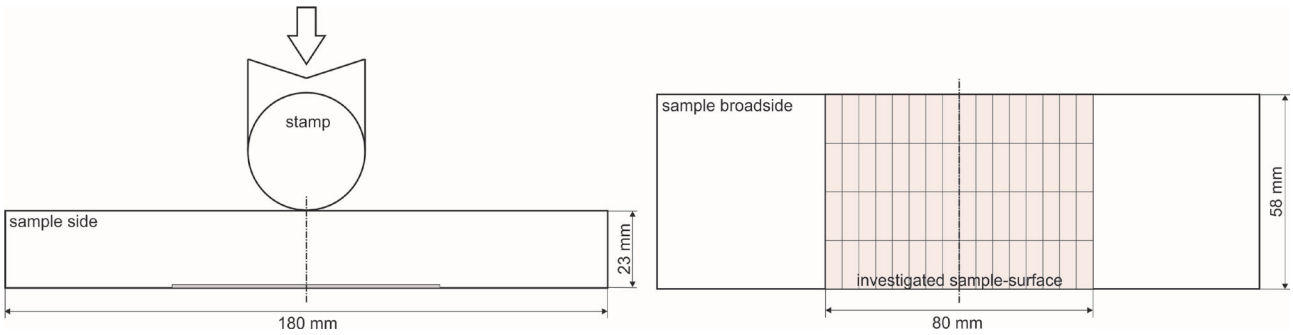

Fig. 4 - Dimensions of investigated area and sample. Left: side view with the bending stamp; right: position of investigated sample area with examination pattern

The physical dimensions of the produced samples are provided in Fig. 4. On the left side, the side view is shown. The sample thickness is 23 mm, width is 58 mm, and length is 180 mm. For a detailed surface investigation, the sample is de-scaled. The strain-influenced area, defined as the region within 40 mm to the left and right of the bending axis, is observed with a stereo microscope in the examination pattern shown in Fig. 4, right. The microscope has a maximum magnification of 62×. This enables the observation of defects with a minimum length of ~50 µm. The cracks are documented and the position and number of each defect is registered. Several cracks are observed in detail with a light microscope and scanning electron microscopy (SEM).

RESULTS

The results of the crack investigations are presented in Fig. 5. The number of cracks is denoted relative to the RA-T curves; the upper line indicates that no cracks occur on the sample surface (circular elements). Every distanced point on this line corresponds to an experimental sample with surface cracks. The number of cracks increases from the top down. The symbols classify the samples in three ranges:

- Circle: no surface cracks; test procedure reveals no risk for transverse cracking
- Triangle: 0 < number of surface cracks ≤ 2 (example: Fig. 6, crack distribution 1); risk for transverse cracking is increasing
- Quadrilateral: >2 surface cracks (example: Fig. 6, crack distributions 2 and 3); high risk for transverse cracking

The leftmost diagram shows the experiments for 0.002 wt.% Nb. The only temperature that triggers the formation of one crack is 850°C. Fig. 6(1) shows the crack position. The essential results are those for 700 to 800°C. No cracks form at this bending temperature range, despite it being the range of the γ-to-α transformation. This is investigated in greater detail with additional experiments later. Increasing the Nb content to 0.02 wt.% reveals a higher number of cracks, as shown in the middle. The high-temperature region of 900 and 950°C is free of surface cracks. At 850°C, the ductility decreases, which causes more cracks to form on the sample surface (distribution (2)). A reduction of the bending temperature improves the behavior; the formation of cracks is slightly decreased. The values for 0.04 wt.% Nb are shown on the right-hand side. The amount of surface cracks increases significantly at this composition. Every sample exhibits at least four cracks. The highest number is found in the samples bent in the high-temperature range. The corresponding crack distribution is presented in **6** on the right side. Decreases in the bending temperature accompany the formation of fewer cracks, but the experimental conditions are obviously much more prone to surface cracking than those with less Nb.

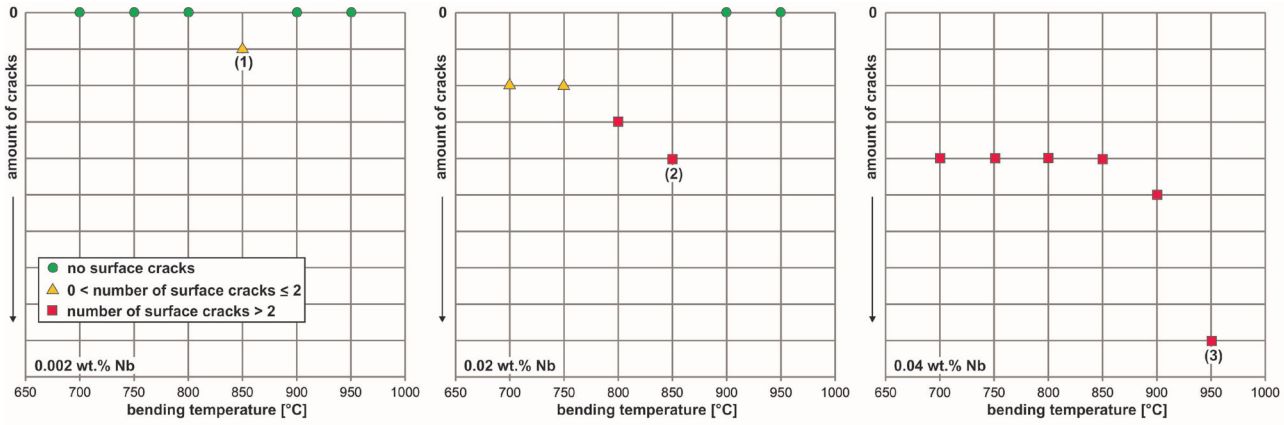

Fig. 5 - Number of surface cracks with respect to steel composition and deformation temperature. Left: Steel 0.002 wt.% Nb, middle: steel 0.02 wt.% Nb, and right: steel 0.04 wt.% Nb

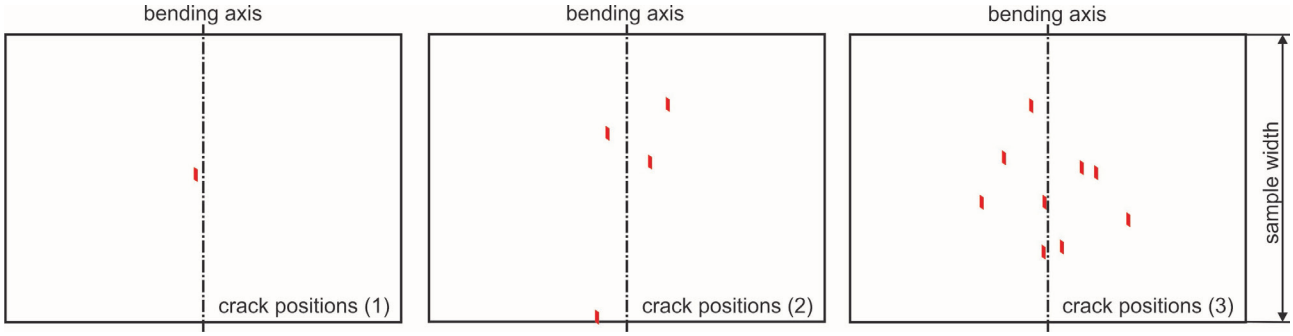

Fig. 6 - Crack distribution examples. Left: Steel 0.002 wt.% Nb, middle: steel 0.02 wt.% Nb, and right: steel 0.04 wt.% Nb

Surface quality of continuous casting products

Fig. 7 shows, on the left side, an example for a crack observed with stereo microscopy. The surface is descaled with a mild treatment. The length of the crack is ~1000 µm. The minimum observed crack length is ~200 µm. Additional investigations on the crack morphology are done using SEM. In Fig. 7, middle, a fine crack along the prior austenite grain boundaries is shown. The grains are very visible, despite the lack of etching treatment. The crack stops at the triple point in the lower region of the picture. The crack length is ~500 µm. The picture on the right side reveals the results of a special crack investigation. A separated small piece, including the surface crack, is cut from the sample. It is notched at the edge opposite the crack and deep-frozen with liquid N_2. The crack is broken under specific force application. Because of the N_2 treatment, the surrounding matrix experiences brittle fracture and the high-temperature crack area can be investigated. A significant advantage of this method is the ability to examine the entire crack area, rather than one section. The picture in Fig. 7 shows a high-temperature crack area. In the lower part, the brittle zone from deep-freeze rupture can be seen. A significant detail is the prior austenite grain boundaries visible in the high-temperature crack area. Also informative is the appearance of scale in the crack. This indicates the high temperature and the presence of scale during cracking. The maximum depth is ~300 µm. The upper part of the picture shows the sample surface with significant roughness, caused by the casting, solidification, and cooling processes.

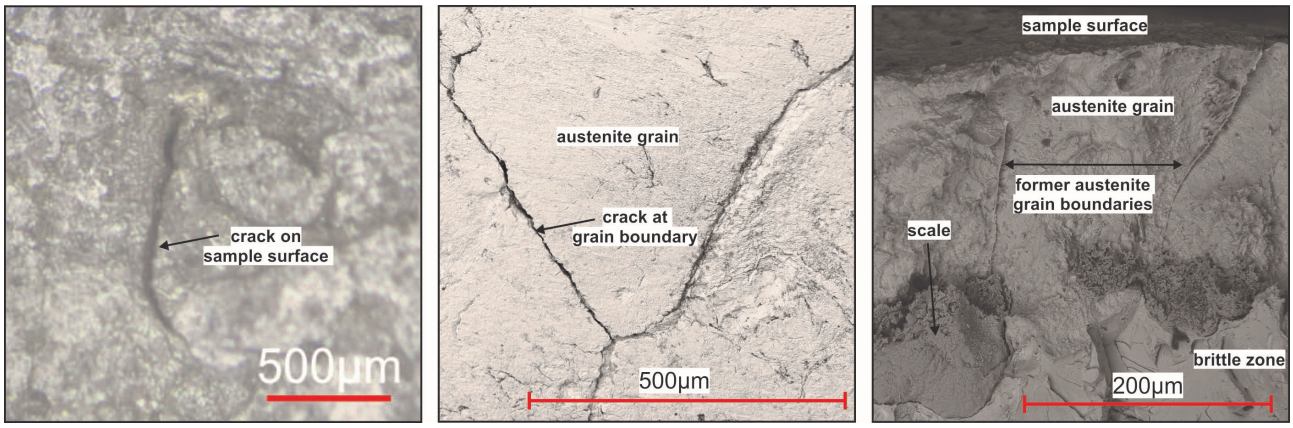

Fig. 7 - Examples of formed cracks. Left: crack on the descaled sample surface, investigated with stereo microscope; middle: crack on the descaled sample surface (SEM); right: ruptured sample with crack formed in the bending experiment and brittle zone

As mentioned in the experimental section, the stamp force was recorded with a processing unit. The values of stamp force can provide much information regarding the high-temperature material behavior. Fig. 8 shows force curves as a function of time.

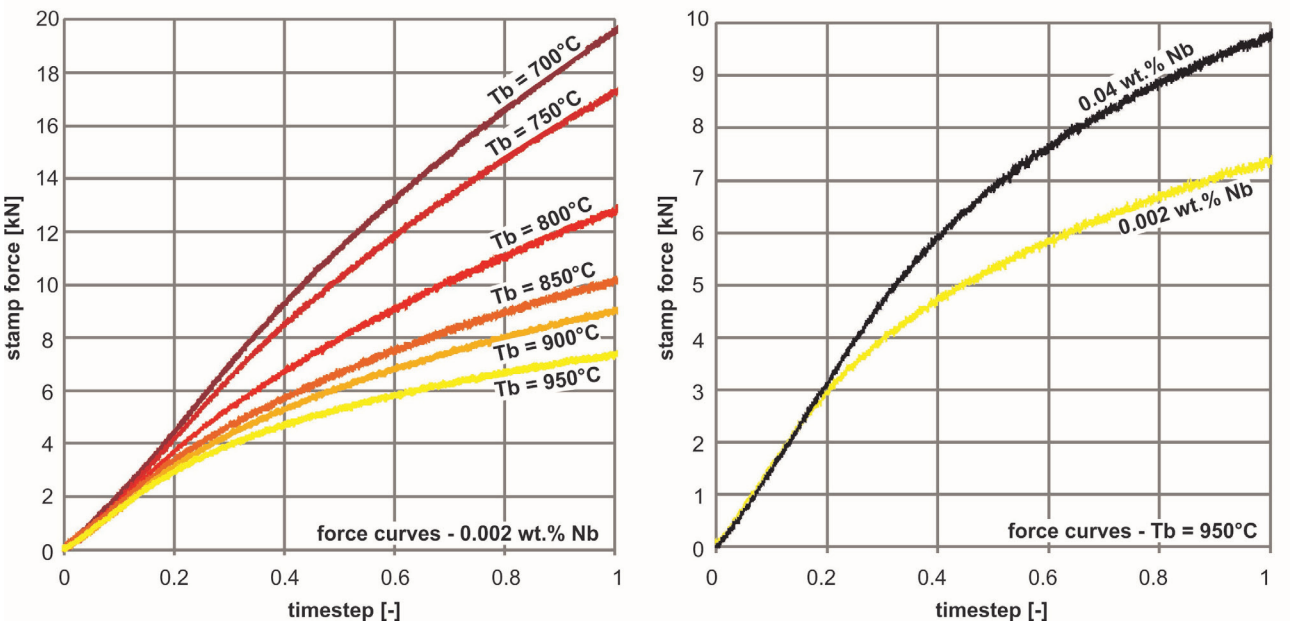

Fig. 8 - Stamp force measurement over time. Left: Influence of the bending temperature on the force curves; right: Influence of steel composition at 950°C

On the left-hand side, curves obtained for the six bending temperatures of the steel with no added Nb can be seen. The influence of the temperature is clearly visible; higher temperatures correlate to lower maximum measured stamp forces. The different gradients indicate that greater plastic deformation occurs at higher temperatures, which are achieved earlier. The small differences in time of ~0.15 can be explained by the changes in the Young's modulus of the steel. The right-hand side shows the influence of the Nb content on the force curves at 950°C. An addition of 0.04 wt.% Nb causes a significant increase in the maximum applied stamp force. The measurements clearly indicate the behavior of the samples during the test and can be used for model optimization in the simulation.

DISCUSSION

The impact of Nb on the formation of surface cracks was obtained clearly. A study by Ouchi and Matsumoto [21] on the hot ductility, investigated through hot tensile testing, also showed the obvious influence of Nb. The addition of Nb in four steps, reaching 0.074 wt.%, significantly decreased the RA value at each step. This is explained by the higher number of Nb(C,N) precipitates at increased Nb contents; these precipitates are located at the austenite grain boundaries, causing high embrittlement. The ductility trough is broadened, particularly at higher temperatures. However, the lowest RA values at the highest Nb content of 0.074 wt.% still occur at temperatures of 800 to 850°C. Compared with the present study with the in-situ hot bending test, the lowest ductility for 0.04 wt.% Nb is examined at the highest bending temperature of 950°C. The differences in the results could be attributed to the total applied strain. In the bending test, the total strain is 1.5%; this value is similar to the strains during unbending. No dynamic recrystallization should occur to recover ductility at higher temperatures. Without recovery, the harmful effects of Nb could be revealed at higher temperatures.
Regarding the steel with 0.002 wt.% Nb, the formation of surface cracks at the maximum strain of 1.5% is not critical. Only at 850°C, one crack forms on the sample surface. It is unclear whether this crack indicates the beginning of a ductility trough. To observe the influence of the induced strain, this steel was further tested with a total strain of 6.5%. Fig. 9 presents the results of this investigation. Again, the formed cracks are counted and plotted as a function of the bending temperature. The ductility trough is very pronounced at the temperatures of 850 and 900°C. The ductility increases at higher temperatures, but at 950°C the number of cracks is only reduced to approximately half in comparison to the sample at 900°C. A clearly improved behavior is observed at 800°C. No cracks are formed at 750 and 700°C. The reason for this significant result could be the precipitation state. The number and size of AlN precipitates, and even deformation-induced precipitates, can influence cracking. This is investigated with further simulations and will be discussed in further publications.

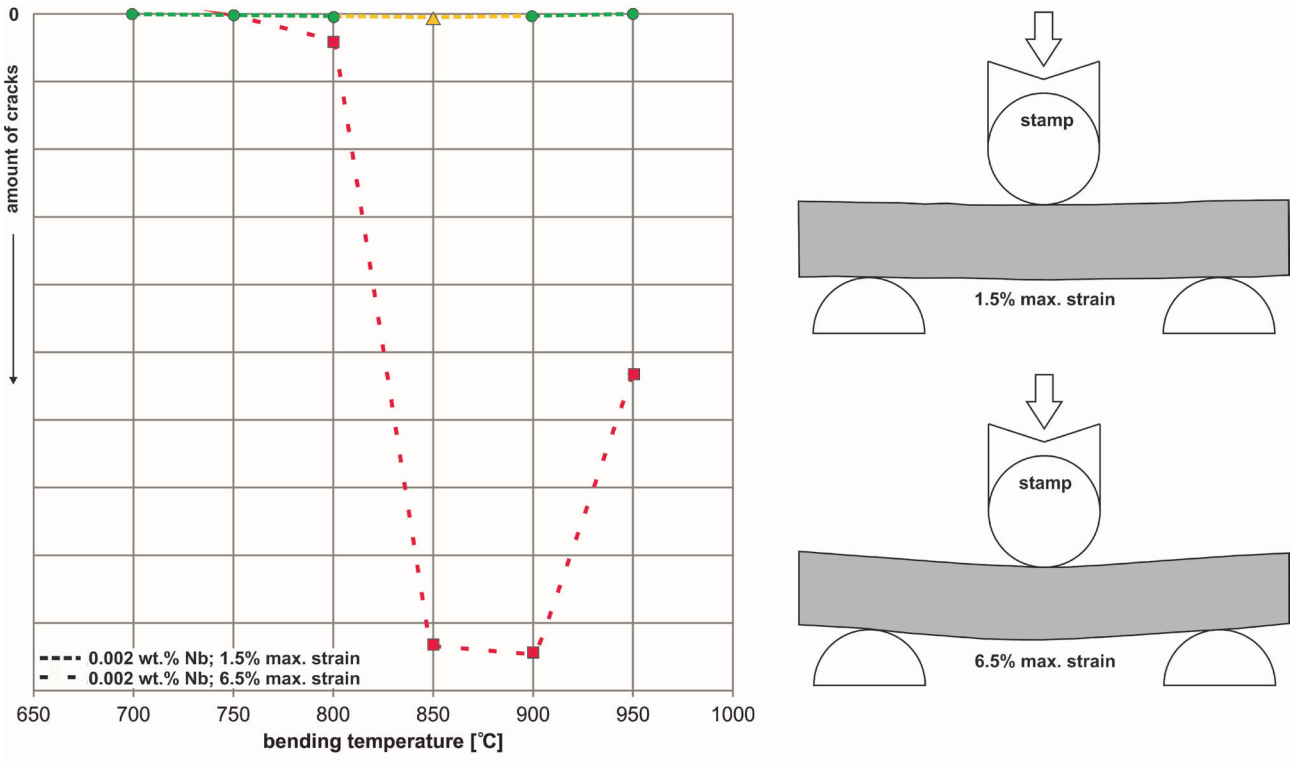

Fig. 9 - Results for the surface crack formation of steel with a Nb content of 0.002 wt.% as a function of the total induced strain (left). Right: deflection at room temperature for 1.5% and 6.5% maximum strains.

The results in Fig.9 at 750 and 700°C are very noticeable. No crack forms at the surface, even under the maximum strain of 6.5%. Theoretically, the ductility is predicted to suffer losses in this temperature region because of the γ-to-α transformation. To determine the A_{R3} temperature, the 700°C sample is investigated with a high-temperature laser scanning confocal microscope (HT-LSCM). This is a useful tool for investigating high-temperature material phenomena, e.g., austenite grain growth or transition temperatures [22]. Therefore, a ground and polished sample is heated to the austenitizing temperature of 1320°C. The thermal etching effect enables the visualization of the microstructure after the new austenite grains have formed. A significant advantage of this technique is the possibility of observations of the early stages of the transition. The phases that appear first can be determined through video studies after the experiment. The high temperature and a holding time of 10 min promote a coarse austenite grain structure, similar to the prior grains in the experiment. The sample is then cooled according to the temporal sequence for a bending temperature of 700°C (Fig.2). Afterward, it is cooled further to observe the continuing transformation.

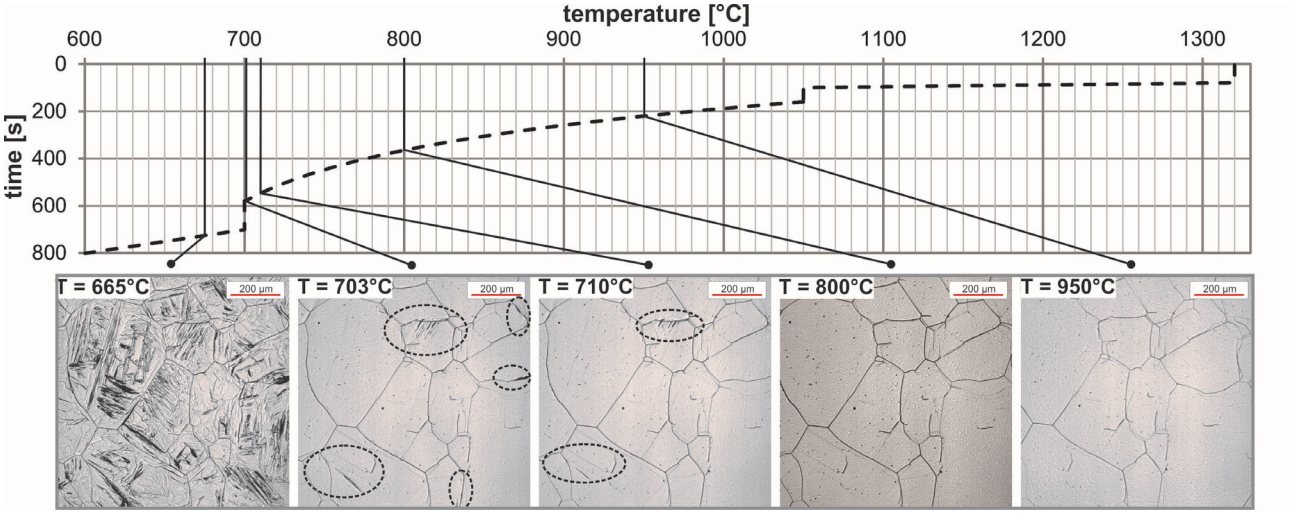

Fig. 10 - Cooling sequence for HT-LSCM investigations. Microstructural pictures during cooling with the first appearing phases.

Fig.10 presents the cooling sequence after austenitizing and the microstructure of the sample at significant temperatures. At 950°C, where the number of cracks is rather high after bending, a fully austenitic structure is visible. After the ductility trough (900 to 850°C) at 800°C, austenite remains as the only present phase. Ferrite phases become visible at approximately 720°C. The micrograph obtained at 710°C shows the start of the transformation at two positions. Obviously, the phases resemble Widmanstaetten-ferrite. In the upper corner of this micrograph, an initial ferrite film can be seen, which becomes much clearer at a temperature of 703°C. The phases grow and the steel transforms at more points, becoming mostly ferrite at the prior austenite grain boundaries. At 665°C, the transformation to ferrite is nearly finished.

These results reveal a certain ferrite phase at 700°C. Deformation-induced ferrite would be present at earlier stages in cooling (750°C), but obviously this has no negative effect on the surface ductility during the experiments. This is a fundamental fact investigated in greater detail in future studies. It demonstrates very well how the two methods of HT-LSCM and IMC-B testing can be used to investigate material behavior at near-reality conditions.

CONCLUSION

The In-situ Material Characterization–Bending test (IMC-B) represents a new testing method for investigations of the susceptibility to surface cracking of steel under continuous casting conditions. It permits a realistic experimental simulation. The testing procedure can be summarized in three parts:

- **Solidification**: The steel melt is adjusted in an induction furnace, where the composition can be freely chosen. It solidifies in a mold with heat transfer controlled by mold coatings. The resulting directional dendrite structure includes typical solidification phenomena (micropores, segregations). The columnar austenite grain structure can be described as well conformed to the strand shell.
- **Controlled cooling**: After stripping of the mold, the cooling is adjusted to a given temporal sequence or cooling strategy, which imposes similarity of the microstructure and precipitation kinetics to that observed in the casting process (with scale formation). The temporal sequence is realized with pyrometer measurements and appropriate furnace temperatures.
- **Deformation with three-point bending**: Deformations of the strand shell are simulated with an isothermal three-point bending test. The defined maximum strain and strain rate on the sample surface is limited to a few percentage points, preventing dynamic recrystallization and minimizing deformation-induced ferrite and precipitates, thereby allowing the simulation of conditions in the unbending zone of the caster.

To determine the influence of Nb on the formation of transverse cracks, a test series with a medium-carbon steel and varied Nb contents was done. To simulate the unbending step in the casting machine, the maximum induced strain was 1.5%. The time sequence until the performance of the bending test (or the start of unbending) was adjusted to match the parameters of a slab caster with a casting speed of 1.2 m/min. The deformation was performed at six temperatures ranging from 700 to 950°C.
The investigations of the deformed sample surface revealed the significant influence of the Nb content on the formation of surface cracks. Starting with a Nb content of only 0.002 wt.% Nb, a single crack formed only at the temperature of 850°C. With 0.02 wt.% Nb in this steel, the number of initiated surface cracks increased. The most critical temperatures were 850 and 800°C, whereas the high temperatures were again free of surface cracks. With 0.04 wt.% Nb, the behavior deteriorated significantly. Every experiment showed at least four cracks, and a significant ductility trough was observed at 950°C. The cause for this high-temperature trough could be the prevention of dynamic recrystallization by the low strain values.
Increasing the maximum strain on the steel with 0.002 wt.% Nb to 6.5% caused a significant increase in surface cracking at 850 and 900°C. This could be attributed to the precipitation state of AlN during bending. At 700 and 750°C, no cracks formed, even under higher strains. Therefore, the steel was investigated with a HT-LSCM under experimental conditions. The micrographs revealed initial ferrite phases forming at approximately 720°C without deformation. The start of the transformation did not damage the surface quality. This result is will be investigated in greater detail in the future.

BIBLIOGRAPHY

[1] J.K. BRIMACOMBE, K. SORIMACHI, Crack formation in the continuous casting of steel, Metallurgical Transactions B, Vol. 8, No. 3, (1977), pp 489.
[2] B. MINTZ, S. YUE, J.J. JONAS, Hot ductility of steels and its relationship to the problem of transverse cracking during continuous casting, International Materials Reviews, Vol. 36, No. 5, (1991), pp 187.
[3] B. MINTZ, The influence of composition on the hot ductility of steels and to the problem of transverse cracking, ISIJ International, Vol. 39, No. 9, (1999), pp 833.
[4] R. DIPPENAAR, S.-C. MOON, E.S. SZEKERES, Strand surface cracks – The role of Abnormally-Large Prior-Austenite Grains, Proceedings AISTech, (2006), pp 833.
[5] E.S. SZEKERES, Overview of mould oscillation in continuous casting, Iron and Steel Engineering, Vol. 73, No. 7, (1996), pp 29.
[6] B. MINTZ, S. YUE: The Hot Tensile test For Assessing the Likelihood of Transverse Cracking During Continuous Casting of Steel, 34th Mechanical Working and Steel Processing Conference, Montreal, Canada, pp 391.
[7] K. SCHWERDTFEGER, Rißanfälligkeit von Stählen beim Stranggießen und Warmumformen, Verlag Stahleisen mbH, Düsseldorf, Germany, (1994).
[8] B. MINTZ, Importance of columnar grains in dictating hot ductility of steels, Materials Science and Technology, Vol. 16, (2001), pp 1.
[9] K. SCHWERDTFEGER and K.-H. SPITZER, Application of Reduction of Area–Temperature Diagrams to the Prediction of Surface Crack Formation in Continuous Casting of Steel, ISIJ International, Vol. 49, No. 4, (2009), pp 512.
[10] C. BERNHARD, P. KRAJEWSKI, T. SCHADEN, S. ILIE, In-situ-Biegeversuch zur experimentellen Simulation der Bildung von Oberflächenrissen im Stranggießprozess, Fachausschuss für physikalische Chemie und metallurgische Verfahrensentwicklung des VDEh, Düsseldorf, Germany, (2014).
[11] B. MINTZ, R. ABUSHOSHA, M. SHAKER, Influence of deformation inducted ferrite, grain boundary sliding and dynamic recrystallization on hot ductility of 0.1-0.75 %C steels, Material Science and Technology, Vol. 9, (1993), pp 907.
[12] D.N. CROWTHER., The Effects of Microalloying Elements on Cracking During Continuous Casting, The Use of Vanadium in Steel - Proceedings of the Vanitec Symposium, Beijing, China, (2001), pp 99.
[13] B. MINTZ, J. LEWIS, J.J. JONAS., Importance of deformation induced ferrite and factors which control its formation, Materials Science and Technology, Vol. 13, (1997), pp 379.
[14] H. PRESSLNGER, M. MAYR, E. TRAGL, C. BERNHARD, Assessment of the Primary Structure of Slabs and the Influence on Hot- and Cold-Rolled Strip Structure, Steel Research Int., Vol. 77, No. 2, (2006), pp 107.
[15] S. ILIE, J. REITER, J. FLUCH, H. PRESSLINGER, C. BERNHARD, Characterization of hot tear segregations in continuous casting of slabs, 6th European Continuous Casting Conference, Riccione, Italy, (2008), pp 122.
[16] J. REITER, C. BERNHARD, H. PRESSLINGER, Austenite grain size in the continuous casting process: Metallographic methods and evaluation, Materials Characterization, Vol. 59, (2008), pp 737.
[17] D.N. CROWTHER, B. MINTZ, Influence of grain size on hot ductility of plain C-Mn steels, Materials Science and Technology, Vol. 2, (1986), pp 951.
[18] D.N. CROWTHER, B. MINTZ, Influence of grain size and precipitation on hot ductility of microalloyed steels, Materials Science and Technology, Vol. 2, (1986), pp 1099.
[19] J.Y. FU., C.I. GARCIA, S. PYTEL, A.J. DEARDO, Hot ductility of continuously cast microalloyed steels, Processing, Microstructure and Properties of HSLA Steels, (1988), pp 27.
[20] P. KRAJEWSKI, R. KROBATH, C. BERNHARD, J. MIETTINEN, S. LOUHENKILPI, S. ILIE, T. SCHADEN, A Novel Approach for the Simulation of Surface Crack Formation in Continuous Casting, BHM, Vol. 160, No. 3, (2015), pp 109.
[21] C. OUCHI, K. MATSUMOTO, Hot ductility in Nb-bearing high- strength steel low-alloy steels, Transactions ISIJ, Vol. 22, (1982), pp 181.
[22] N. FUCHS, P. KRAJEWSKI, C. BERNHARD, In-situ Observation of Austenite Grain Growth in Plain Carbon Steels by Means of High-temperature Laser Scanning Confocal Microscopy, BHM, Vol. 160, No. 5, (2015), pp 214.